Faraday Rotation Modulators for mm-Wavelength Polarimetry

Brian G. Keating

ABSTRACT

The design and performance of wide bandwidth linear polarization modulators based on the Faraday effect in corrugated cylindrical waveguide is described. The device can be used as a polarization modulator for millimeter-wave and microwave polarimetry and is functionally similar to a birefringent crystal waveplate, but with no moving parts. The Faraday rotation modulator's intrinsically single-moded design results in wide-bandwidth performance with low-loss, and is capable of polarization modulation up to ~ 10 kHz. The Faraday Rotation Modulator is capable of operation at cryogenic temperatures and is scalable for use up to electromagnetic frequencies of 300 GHz. Faraday rotation modulators operating at 100 and 150 GHz, with 30% fractional bandwidths in each band have been used to make astronomical observations of polarized galactic emission.

1. INTRODUCTION AND MOTIVATION

Measurements of the polarization of the cosmic microwave background (CMB) have the promise to revolutionize our understanding of the early universe. Unlike the temperature anisotropy of the CMB, which has been measured to exquisite precision over a wide range of angular scales, the polarization of the CMB has only recently been detected and remains relatively unexplored. To detect the faint CMB polarization it will also be necessary to detect and remove polarized galactic emission from interstellar dust and synchrotron sources which can be accomplished if polarimetry is done in multiple millimeter-wave bands.

Polarimeters often employ mechanisms to modulate the plane of polarization of the incident radiation field about the optical axis. In conjunction with an analyzer (to decompose the radiation into orthogonal polarization states), a modulator is used to exchange the polarized intensity between the two detectors (or two orientations of a single detector). If the modulation is done rapidly enough, this technique mitigates the effects of detector gain instability. If the detector's gain instability systematics are mitigated by other means, e.g. spatial scanning, then the FRM can be used in a "point-and-integrate" mode where it is used solely to modulate polarization. This can simplify either the optics, detectors (allowing for only one linear polarization state to be detected) or the telescope's mount. In such situations, having both FRM and scanning modulation, allow the tasks of beam systematics mitigation and detector fluctuation systematics mitigation to be separated.

1.1 Polarization modulation

Traditionally, polarization modulation for millimeter-wave polarimeters was accomplished by physical rotation of the polarimeter about the optical axis,[1,2] mechanical rotation of a waveguide polarizer,[3] rotation of a wire grid polarizer,[4] or rotation of a birefringent half-waveplate.[5,6] In many CMB experiments, polarization modulation is often effected by parallactic angle rotation ("sky rotation") with respect to the instrument coordinate system.

Classical polarization modulation mechanisms often employ bulky and complex mechanisms which are subject to failure with repeated use. The modulators described in this paper represent a novel approach to the technology of CMB polarization modulation. Early CMB polarimeters (including Penzias and Wilson's, which *was* polarization-sensitive) used a combination of sky-rotation with rotation of the entire telescope to modulate CMB polarization. These experiments[7,8] rotated hundreds or thousands of kilograms, were susceptible to vibration induced microphonic noise, and were limited mechanically to modulation rates < 0.1 Hz.

The next polarization modulation innovation was a birefringent half-waveplate: a single crystal of anisotropic dielectric (typically quartz or sapphire) that phase-delays one of the two linear polarizations.[4,9] While the fragile ~ 1 kg, cryogenically-cooled crystal *can* be rotated at ~ 10 Hz with lower-vibration than rotation of the entire

Brian Keating is with the Department of Physics, University of California, San Diego, La Jolla, CA 92093-0424 USA.

telescope, such a mechanism is prone to failure since bearing operation is a severe challenge at cryogenic temperatures. And since bolometers are sensitive to power dissipation at the 10^{-17}W level, even minute mechanical vibrations produced by the bearings are intolerable.

The Faraday Rotation Modulator [†](FRM) shown in Figure 1, requires only "rotating" electrons (the generation of a solenoidal magnetic field) in a magnetized dielectric to effect polarization rotation. Therefore, FRMs reduce the rotating mass that provides modulation by 30 orders of magnitude! Furthermore, these devices are capable of rotating polarized millimeter wave radiation at rates up to 10 kHz—faster than any conceivable time-varying temperature- or optical-gain fluctuation. A superconducting NbTi solenoid wound around the waveguide provides the magnetic field that drives the ferrite into saturation, alternately parallel and anti-parallel to the propagation direction of the incoming radiation. The FRM rotates the CMB polarization vectors by $\pm 45^\circ$ at 1 Hz, well above 1/f-fluctuation timescales (caused by, for example, temperature variations). The Polarization Sensitive Bolometer (PSB) signals are detected using phase-sensitive amplification phase-referenced to the solenoidal field drive waveform.

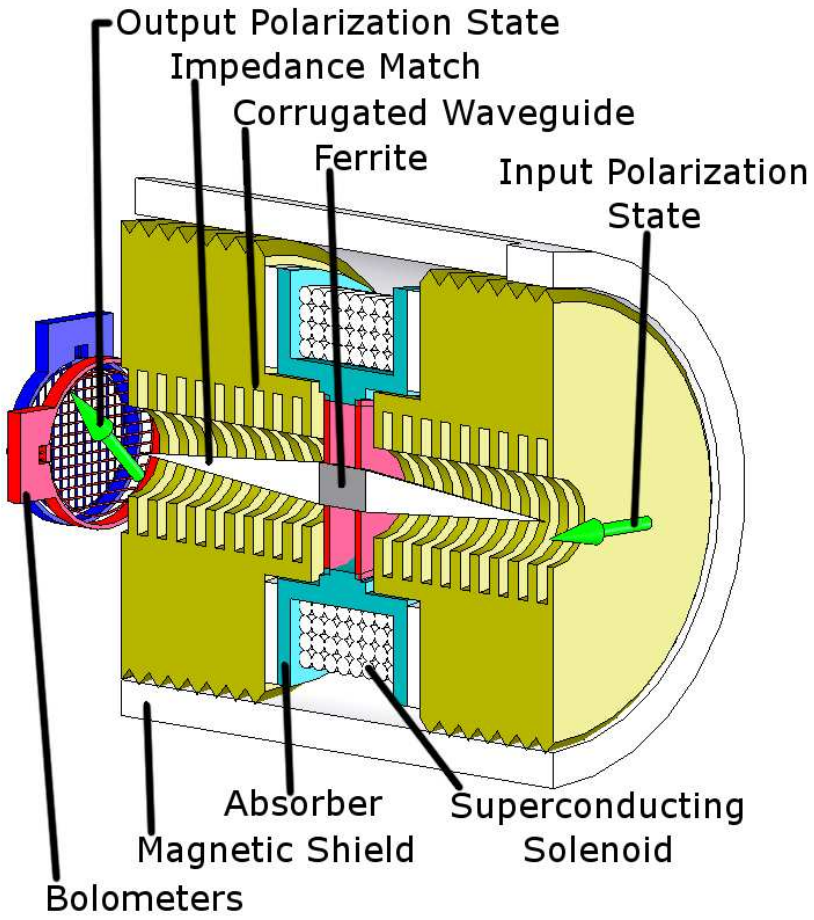

Figure 1. A cross-sectional view of a Faraday Rotation Modulator (FRM) pixel. Polarized light enters from the right, is rotated by $\pm 45^\circ$ and then analyzed (decomposed into orthogonal polarization components, which are detected individually by the polarization-sensitive bolometers, or PSBs). For each FRM pixel, the PSBs are contained within a corrugated feedhorn, cooled to 0.25 K, located approximately 20 cm from the FRM, which is placed in a corrugated waveguide at the interface between two corrugated feedhorns, placed back-to-back and cooled to 4 K – see figure 2. The (schematic) location of the PSBs in this figure serves to illustrate the coordinate system used as the polarization basis. Figure credit: Thomas Renbarger.

[†]US Patent Pending: "Wide Bandwidth Polarization Modulator, Switch, and Variable Attenuator," US Patent and Trademark Office, Serial Number: 60/689,740 (2005)

Faraday Rotation Modulators, like waveplates, have the promise to mitigate optical systematic effects occurring "downstream" from the modulator. Though the FRMs described in this work operate in waveguide, following the primary aperture of the telescope and additional coupling optics, nevertheless the Faraday effect could also be able to be implemented in free-space, perhaps at a cold optical stop. In such an implementation the polarization modulation would be identical to a birefringent waveplate, except that *no* mechanical rotation mechanism would be required.

In free space, or in waveguide, Faraday modulation of the plane of polarization can be effected in a continuous modulation mode or in a step-and-integrate mode. In either mode the effective polarization angle can be commanded with extremely high precision and repeatability which also obviates the need for a servo system as used in a conventional half waveplate modulation.

The Faraday effect in waveguide has also been used to rotate millimeter-wave polarization between two fixed states -90° and $+90^\circ$. Such a mode is equivalent to a 180° phase switch. This implementation has been successfully deployed in the MBI experiment and is further described in this volume.[10]

In November 2005 a millimeter-wave polarimeter with 49 spatial pixels was deployed to the United States' Amundsen-Scott South Pole Station. This CMB polarimeter called BICEP[2,8] required low-systematic, high-reliability, polarization modulation. This led to development and observations with the FRMs as a secondary form of polarization modulation (the primary modulation mechanism being rotation of the BICEP telescope about its boresight axis).

The FRM provides rapid modulation of the plane of linear polarization (the dominant type of CMB polarization) and was operated in a continuously switching mode (as opposed to a continuously rotating mode or a "point-and-integrate mode"). In the continuously switching mode the Stokes parameter measured by a paid of linearly polarized detectors is switched between +Q and -Q. Only the polarized component of the incident flux is modulated and subsequently analyzed with phase-sensitive detection (lock-in amplification). In the BICEP experiment six FRMs; three operating at 100 GHz and three at 150 GHz, were deployed as a proof-of-concept test of the FRM technique and to explore operational modes for this new device. Preliminary results from BICEP's FRMs are discussed below.

In the 1970's a polarimeter which used a Faraday modulator and an orthomode transducer as a polarization analyzer was employed by Nanos[11] to conduct early studies observations of the CMB. The modulator described in this white paper (Fig. 1 has a bandwidth $\simeq$ 30 times greater than Nanos' or those currently available from commercial vendors such as MPI/QuinStar Technology Inc. Our devices are also capable of operation at cryogenic temperatures, which is an operational advantage not enjoyed by Nanos' devices nor commercially available devices.

2. DESIGN

The magneto-optical design of the modulator is based on a room temperature isolator employing a ferrite dielectric waveguide[12] and a cryogenic isolator.[13] These isolators operate in rectangular waveguide allowing precise mode filtration and low spurious mode generation. Operation as a polarization modulator requires matching modal propagation coefficients of the propagating modes in the entrance waveguide (TE_{10}, TE_{11}°, or HE_{11}°) and the propagating HE_{11}^{diel} mode in the dielectric guide. For the tests described in this paper a corrugated circular waveguide with a 2.35 mm diameter was used. The Faraday modulator design is displayed in Fig. 1.

To achieve magnetic saturation with low Joule heating, a solenoid constructed of superconducting copper niobium wire is used. According to the manufacturer of the ferrite this material has a saturation magnetization of $4\pi M_z = 5000$ gauss which is obtained with an applied magnetic field of $H \simeq 30$ Oe. This field is produced by the superconducting solenoid with $N \sim 200$ amp-turns. The calculated self inductance of the solenoid is $L = \mu_o N^2 A/\ell = 10$ mH where A and ℓ are the area and length of the solenoid. This value agrees well with the inductance measured with an LCR meter and directly by observing the L/R time constant of the solenoid at 4 K. All performance attributes of the modulator are improved with careful attention to assembly details and tolerances. In particular, the alumina cone-ferrite cylinder "toothpick" assembly must be placed along the propagation direction with less than 1° tilt, otherwise resonant mode conversion produces several dB of insertion loss.

3. POLARIMETRY WITH FARADAY ROTATION MODULATORS

Figure 2 is a schematic illustration of a FRM as implemented in a bolometric polarimeter. Bolometric polarimeters, such as BICEP[2] often utilize a back-to-back corrugated feedhorn geometry to provide (electromagnetic interference) EMI shielding between the beam-defining optics (typically cooled to $\simeq 4.2$ K)and the detector coupling optics (typically < 0.3 K). The EMI shield is implemented as a high-pass filter (waveguide choke) between the two back-to-back feedhorns in the beam-defining optics section, preventing radiofrequency radiation from being detected by the high-impedance bolometers. The waveguide choke allows a single waveguide mode to propagate, and it is here that the FRM is installed.

Detection after modulation can be accomplished with a bolometric or HEMT amplifier radiometer. For the latter application, the rapid modulation frequencies available with the Faraday rotator allows the radiometer to be Dicke-switched in total power mode, *i.e.*without other forms of phase modulation. The FRM polarimeter, whether used with a HEMT amplifier or bolometer detector system, completely characterizes the linear polarization state of the incident radiation from the same spatial pixel in the focal plane of a telescope. This allows the incident radiation in each linear polarization state to propagate through the same optical train (windows, lenses, filters, detectors), under identical optical loading conditions. Unlike polarization modulation by physical rotation of the polarimeter, polarimeters employing FRMs allow the polarization to be modulated without moving the telescope's antenna beam on the sky. By keeping the spatial beam pattern fixed on the sky we isolate the polarization properties and can ignore variations of the beam response or excess variable pickup from the ground.

We used a pair of polarization sensitive bolometers (PSBs) to simultaneously analyze (separate the incident beam into orthogonal polarization states) and detect the power in each state.[14] For an incident electric field

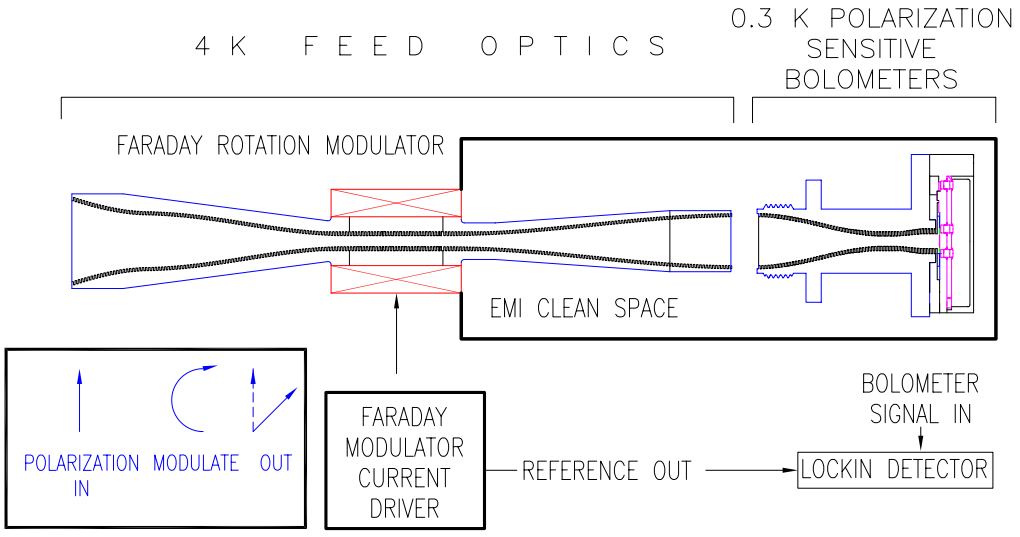

Figure 2. Conceptual schematic of a Faraday polarization modulator coupled to a polarization sensitive bolometer (PSB) used as a polarimeter. The modulator is placed at the waveguide choke and rotates the plane of linear polarization of the propagating HE^{11} spatial mode.

described by

$$\begin{aligned}\overrightarrow{E}(x,y,z,t) &= E_x(t)\sin\left[2\pi\left(\frac{z}{\lambda}-\nu t\right)+\phi_x(t)\right]\hat{\mathbf{x}} \\ &\quad +E_y(t)\sin\left[2\pi\left(\frac{z}{\lambda}-\nu t\right)+\phi_y(t)\right]\hat{\mathbf{y}}, \end{aligned} \tag{1}$$

time-averaging over the electric field oscillations, the Stokes parameters of this field are defined as:

$$I \equiv \langle E_x^2\rangle + \langle E_y^2\rangle, \tag{2}$$

$$Q \equiv \langle E_x^2\rangle - \langle E_y^2\rangle, \tag{3}$$

$$U \equiv \langle 2E_xE_y\cos(\phi_x-\phi_y)\rangle, \tag{4}$$

$$V \equiv \langle 2E_xE_y\sin(\phi_x-\phi_y)\rangle, \tag{5}$$

where I is the intensity, Q and U describe the linear polarization, and V quantifies the circular polarization of the electric field. The CMB is linearly polarized so $V = 0$. If the source is a blackbody radiator in the Rayleigh-Jeans portion of the spectrum, then the observed Stokes parameters are $I \propto (T_x + T_y), Q \propto (T_x - T_y)$ with the proportionality constants fixed by calibrating the receiver system.

The signal produced by differencing the two linear polarization-sensitive bolometers when the microwave signal is Faraday modulated is

$$V_{diff} = S \times \eta_{opt}\eta_{pol}[Q\cos 2\theta(t) + U\sin 2\theta(t)] \tag{6}$$

where the (time dependent) modulation angle is

$$\theta(t) = B_z(t)\gamma l\sqrt{\epsilon}/2c, \tag{7}$$

and l, ϵ, γ, and S are the ferrite's length, dielectric constant ($\simeq 12$), gyromagnetic ratio of the electron, and the bolometric sensitivity in V/W, respectively. $B_z(t) = H_z^{app}(t) + 4\pi M_z(t)$ is the (time-dependent) magnetic induction.

4. PERFORMANCE

In order to be useful as a linear polarization modulator the FRM must rotate mm-wave radiation with high modulation efficiency, low loss, and little degradation of polarimetric fidelity. We divide the performance criteria into four classes (electromagnetic, thermal, modulation, polarization systematics). When multiple devices are used, as with BICEP, we must ensure that the devices are matched in performance and have reasonable operating requirements. To determine if the FRMs could achieve these goals, extensive testing on individual devices (as in Fig. 2) at room temperature, and on arrays of FRMs at cryogenic temperatures (4.2 K) were performed.

4.1 High-Frequency Electromagnetic Performance

Faraday rotation modulator was constructed for use with polarization sensitive bolometers over the frequency range 80 to 110 GHz. Figure 3) shows the insertion and reflection loss of the rotator versus frequency measured at room temperature on a vector network analyzer (VNA). Rectangular-to-circular transitions were used to couple power from the VNA to the waveguide ports of the FRM. Excellent agreement was found between its measured and performance simulated using Ansoft's High Frequency Structure Simulator. The average microwave transmission efficiency of the rotator is 80% and the band-averaged reflection loss is less than 1% across a 27 GHz band (28% fractional bandwidth). Similar devices operating from 130-215 GHz have been produced, and 49 devices operating in the 100 and 150 GHz bands have been cooled to 4.2 K and used as polarization modulators.

4.2 Polarization Modulation Performance

To determine the Faraday rotator's suitability for use as a polarization modulator, a 80-100 GHz bolometric test receiver was constructed. The receiver consists of a corrugated feedhorn, Faraday modulator and polarization sensitive bolometers operating at 0.3 K, as shown in Fig. 5. The bolometers were calibrated using unpolarized thermal loads and the receiver was configured to view a 100% polarized source produced by a wire grid polarizer and a 300 K load reflected from the grid and 77 K transmitted through the grid. This source presents a 100% polarized signal with an antenna temperature of 223 K into the receiver which was subsequently modulated by the Faraday rotator.

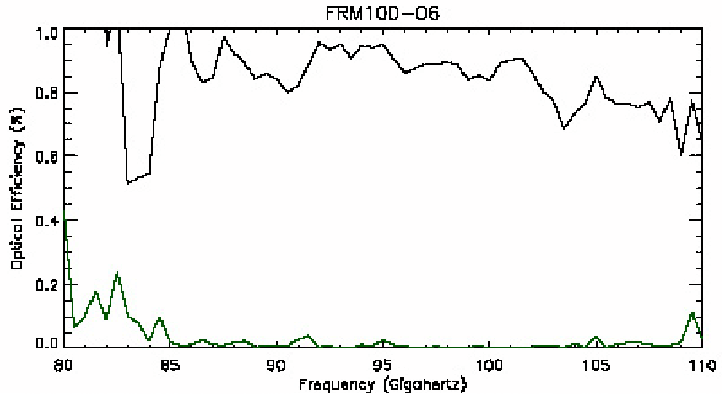

Figure 3. Optical efficiency (transmission) measurements of a 100 GHz Faraday rotation modulator at 300 K measured on a vector network analyzer. The band-averaged transmission for the modulator is 80% warm, and improves to approximately 85% when cooled below 10 K. The reflection (black) and absorption (green line) features at 83 GHz are arbitrary and determined by the desired high-pass cutoff frequency of the corrugated waveguide.

4.2.1 Rotation Angle

The Faraday rotator's polarization rotation angle was determined using a polarizing grid. The FRMs were confirmed to continuously rotate polarized millimeterwave radiation by as much as 160°.

To determine the rotation angle, the maximum and minimum detector output voltages were determined. Since the PSBs are absorbing polarization analyzers, a maximum voltage is produced when the wire-grid axis is oriented perpendicular to the bolometer's sensitivity axis. The bolometer's voltage is minimized when the grid azimuthal angle is rotated by 90° from the maximum. If the grid is positioned midway between the two bolometers, then the polarization rotation angle is given in terms of the bolometer output voltage by:

$$\Theta = \frac{1}{2}\arcsin\Big(\frac{V-(V_{max}+V_{min})/2}{(V_{max}-V_{min})/2}\Big), \tag{8}$$

where V_{max}, V_{min} are the maximum and minimum signal voltages recorded during complete polarization modulation.

4.2.2 Modulation Modes: Continuous Polarization Angle Rotation vs. Switched/Stepped Rotation

From equations 3 and 4 we see that when the electric field produced by the grid is at 45° to each bolometer, $Q = 0$ and U is maximized. If the Faraday modulator is then driven into saturation to rotate the incident polarization angle by +45°, the Stokes parameters (in antenna temperature units) will be $Q = 223K$ and $U = 0K$.

If the current is sinusoidally varied up to the current required for magnetic saturation: $I = I_{sat}\sin\omega t$, the rotation angle will be $\theta(t) = \Theta_o \sin\omega t$ where $\Theta_o = M_{sat}\gamma l\sqrt{\epsilon}/2c$ is in radians, and the difference between the (orthogonally polarized) bolometer signals $V_{x,y}$ is:

$$\begin{aligned}
\Delta V(t) &= V_x - V_y \\
&\propto \cos^2\big(\frac{\pi}{4} - \Theta_o \sin\omega t\big) - \cos^2\big(\frac{\pi}{4} + \Theta_o \sin\omega t\big) &(9)\\
&= \sin(2\Theta_o \sin\omega t). &(10)
\end{aligned}$$

Figure 4 shows sample waveforms for three different magnetic bias values (polarization rotation angles).

Phase sensitive demodulation of $\Delta V(t)$ at the current bias frequency, ω, produces a signal:

$$S = \int_0^{\pi} \Delta V(t) \sin \omega t dt = \int_0^{\pi} -\sin\left(2\Theta_o \sin \omega t\right) \sin \omega t dt$$
$$= g J_1(2\Theta_o) \tag{11}$$

where $J_1(x)$ is the first-order Bessel function and g accounts for the gain of the lock-in (and numerical factors). As shown by Nanos,[15] S is maximized when $\Theta_o = 52.7°$. Since $\Delta V(t)$ is not a pure sinusoidal signal, higher (odd) harmonics are also present, decreasing as $J_n(2\Theta_o)$. For BICEP however, we chose to modulate in a switched mode where the polarization was rotated by $\pm 45°$, having the effect of switching between the Stokes parameter $\pm Q$ in the bolometer coordinate system.

Taking the difference of the bolometer signals is a measure of the value of the Stokes Q parameter (in the coordinate system defined by the two bolometers). As the grid rotates the difference signal varies exactly as in equation 6, with $\theta(t)$ equal to the azimuthal angle of the grid about the optical axis. This measurement describes the detection of linearly polarized radiation with 100% polarization modulation efficiency (in the sense that no other modulator can produce a larger differential signal).

4.3 Polarimetric Fidelity

Three primary systematic effects corrupt polarimetry: instrumental polarization, cross-polarization, and depolarization. Instrumental polarization (IP) results from spurious coupling of the polarimeter (modulator, analyzer, and detectors) to unpolarized radiation. The IP for the bolometric receiver shown in Fig. 5 (with the polarizing grid removed) was determined by observing unpolarized thermal loads (either 300 K or 77 K) and measuring the bolometer difference signals produced as the Faraday modulator was square-wave biased at $\sim$ 1Hz. If there is non-zero instrumental polarization produced by either the optical system and/or the FRM , the two orthogonal bolometer signals will be 180° out of phase, and the amplitude of the bolometer signals will scale with the load temperature. The sum of optical and electrical (cross-talk) IP contributions of the polarimeter has been limited to $< 2\%$ for FRMs used in BICEP.

Instrumental polarization can arise from asymmetry in the toothpick structure. Asymmetries arise both in the construction of the toothpick and its placement in the waveguide. Both the tilt of the toothpick and its concentricity in the waveguide must be controlled to minimize spurious mode conversion from the desired HE^{11}

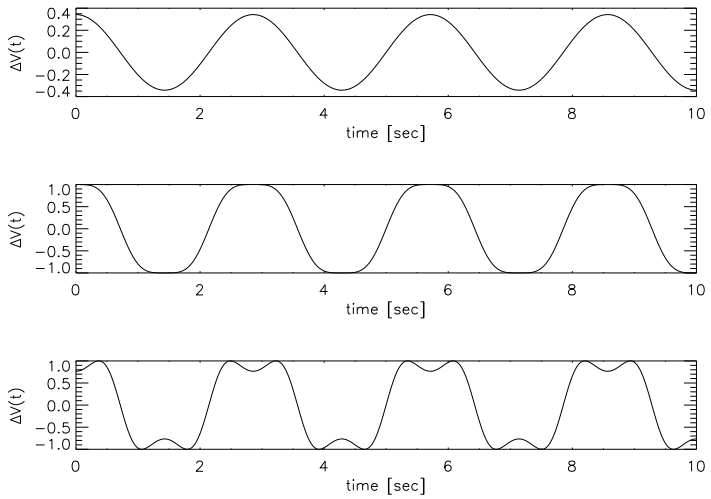

Figure 4. Simulated difference signals (Eq. 10) for orthogonally polarized bolometers viewing a polarized source whose polarization plane is rotated using a Faraday modulator. The bias modulation waveform for all curves is a 2.2 Hz sinusoid with current amplitude set to rotate linear polarization by 10° (top), 45° (middle), and 65° (bottom).

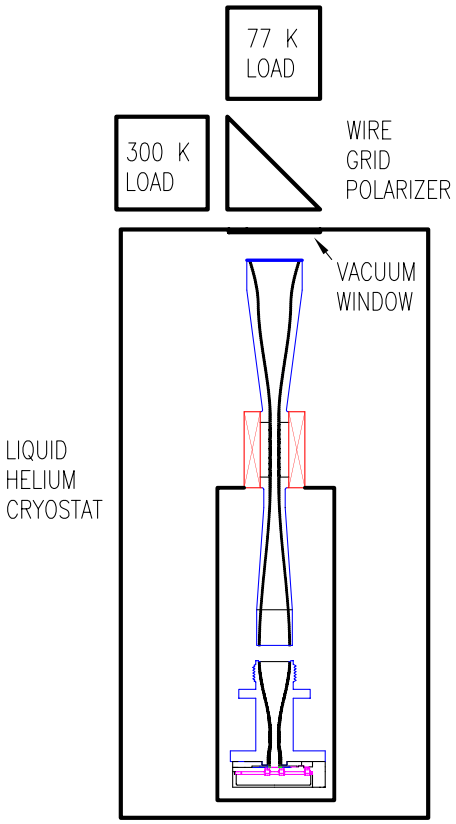

Figure 5. Test set-up for polarization modulation angle, modulation efficiency, and instrumental polarization measurements. Two polarization-sensitive bolometers view a 100% polarized thermal load produced by a wire-grid polarizer tilted at 45° with respect to the optical axis. For measurements of instrumental polarization, the grid is removed and different temperature loads are viewed.

mode to higher order modes. Mode conversion produces differential transmission of the two (degenerate) HE^{11} polarization states, resulting in IP. The alumina cones are manufactured with 0.5° tilt and the ferrite cylinder faces are parallel to better than 0.1°. The assembled toothpick is then placed concentrically in the corrugated waveguide.

When viewing unpolarized thermal loads at 300 K, 77 K, and $\sim$ 12K the IP signals can be seen in real time when the FRM is AC biased. The observed $\sim$ 1% instrumental polarization is consistent with HFSS simulations of the FRM with a $\sim$ 0.5° tilt of the ferrite/alumina toothpick with respect to the corrugated waveguide axis. Since the level IP is constant in time and spatially fixed with respect to the feed and detectors, unlike a polarized celestial source, it can be removed with high-precision. Cross-polarization measurements are also in agreement with HFSS simulations and are consistent with non-orthogonality of the PSBs at the $< 1°$ level.

Depolarization arises due to differences in loss between the two helicity states which propagate in the ferrite. The two helicity states can be written in terms of the linear polarization states as: RCP $= (E_x\hat{\mathbf{x}} + iE_y\hat{\mathbf{y}})/\sqrt{2}$ and LCP $= (E_x\hat{\mathbf{x}} - iE_y\hat{\mathbf{y}})/\sqrt{2}$.

At the operating frequencies of interest ($\sim$ 100 GHz) – well-above the Larmor resonance frequency of saturated TT2-111 ferrite ($\simeq$ 11 GHz) – the difference in attenuation coefficients between the two helicity states is $\alpha_+ - \alpha_- <$ 0.001 Np/m. This implies that RCP electric fields are attenuated by $e^{\alpha_+} = 0.9968$ and LCP fields are attenuated by $e^{\alpha_-} = 0.9964$. This differential attenuation therefore results in *depolarization* (as opposed to *instrumental*

Table 1. Measured properties of 100 and 150 GHz Faraday Rotation Modulators.

Property	Value
Absolute RF Transmission (Warm)	80%
RF Reflection (Warm)	$< 3\%$
Current Required for $\pm 45^\circ$ Rotation	± 130 mA
Power Dissipation (4 K)	$\simeq 1$mW
Polarization Modulation Efficiency (4.2 K)	$\simeq 99\%$
Intrinsic Instrumental Polarization (4.2 K)	$< 2\%$
Cross-polarization (4.2 K)	$< 1\%$
Depolarization (4.2 K)	$< 1\%$

polarization). The polarimeter's signal is the difference between the power in each polarization state, which is proportional to the difference in intensity between the orthogonal polarizations (which is also proportional to the Stokes Q parameter). So

$$Q = |E_x^2| - |E_y^2| = 2\text{LCP} \times \text{RCP}$$

implying $Q_{out} = 0.993\, Q_{in}$ and $U_{out} = 0.993\, U_{in}$. This shows that the polarization angle

$$\tan^{-1} Q_{out}/U_{out} = \tan^{-1} Q_{in}/U_{in},$$

which implies that the output polarized intensity is 99.6% of the input and there is no cross polarization (spurious rotation between $E_x\hat{\mathbf{x}}$ and $E_y\hat{\mathbf{y}}$ or, therefore, between Q and U).

All three polarimetric systematics have been found to be stable over, at least, week-long time periods. This is not surprising as the three systematic effects are intrinsic to the materials used and/or caused by the construction. The stability of these offsets allows them to be modelled and subtracted from the data.

4.4 Magnetothermal Performance

The Faraday modulator uses a superconducting solenoid that requires a magnetic bias $H_{applied} \simeq 30$ Oersted. Large variations in the magnetic field can produce eddy current heating. Careful thermal and magnetic design is therefore required to minimize eddy currents induced in the modulator. In general, eddy current heating effects are proportional to the sample area transverse to the applied magnetic field. For a solenoid made with copper magnet wire, Joule heating of the coil dominates the electromagnetic loss. Eddy current dissipation in the metallic waveguides is ten times smaller than the coil dissipation ($\sim 200\mu$W) for a solenoid that produces the ~ 30 Oersted field required to saturate a 5 Hz sinusoidally-biased ferrite. For a perfect superconducting coil, the coil loss is zero and the total modulator eddy current heating scales as the modulating frequency squared. Simulations using Ansoft's Maxwell SV are in excellent agreement with measurements of the eddy current dissipation of the Faraday modulator from DC to 20 Hz. Magnetic shielding of the bulk experimental volume/bolometers is accomplished by enclosing the solenoid in a high magnetic permeability jacket fabricated from Cryoperm 10.

4.5 Observations of galactic polarization using Faraday Rotation Modulators

The faintness of the CMB polarization signal demands exquisite control of instrumental offsets. There are two ways to mitigate offsets: (1) minimize the offset and (2) modulate the signal before detection (Dicke switch) faster than the offset fluctuates. The BICEP experiment[2] does both. A bridge-circuit differences the two PSBs within a single feed, producing a (first) difference signal that is null for an unpolarized input. This minimizes the offset. For six of BICEP's 49 spatial pixels, the polarized signal input is rapidly modulated (second difference) by Faraday Rotation Modulators (FRM) that rotate the plane of linear polarization of the incoming radiation. The FRMs make use of the Faraday Effect in a magnetized dielectric. Polarization modulation allows the polarized component of the CMB to be varied *independently* of the temperature signal, allowing the response of the telescope to remain fixed with respect to the (cold) sky and (warm) ground. This two-level differencing scheme allows for two levels of phase-sensitive detection, allowing optical systematic effects, associated with the telescope's antenna response pattern (which could leak the much-larger CMB temperature signal to spurious CMB polarization), to be distinguished from true CMB polarization.

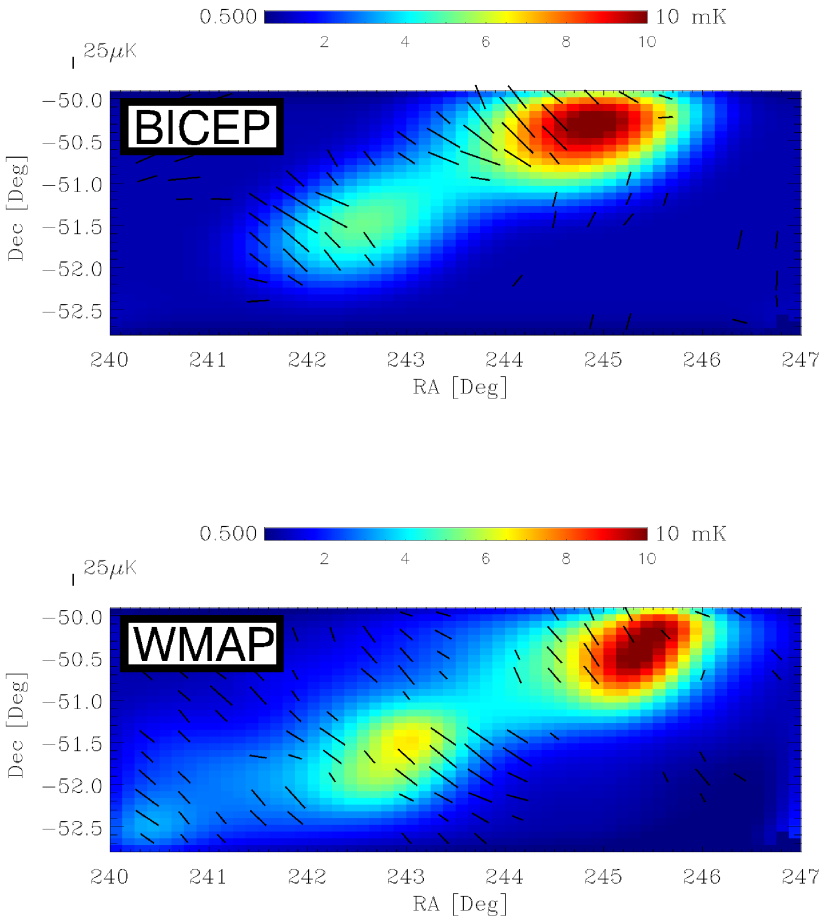

Figure 6. Map of a portion of the galactic plane made using one of BICEP's six Faraday Rotation Modulator (FRM) pixels (top) operating at 100 GHz, compared to WMAP's observations of the same region (bottom). Microwave radiation is polarized by dust grains preferentially aligned by the galaxy's magnetic field. The FRM pixels modulate only the polarized component of the emission and can fully characterize linear polarization *without* rotation of the telescope. The short lines indicate the magnitude and orientation of the plane of polarization, and the color scale indicates the temperature range. For comparison, a scale bar representing 25 μK linear polarization is shown. The galactic plane extends approximately from the lower left to the upper right of each map. Both maps show significant linear polarization orthogonal to the galactic plane.[16] Similar maps were produced for BICEP's 150 GHz FRM pixels. We note that the BICEP FRM data were acquired over the course of only a *week* of observations. Figure credit: Evan Bierman.

BICEP conducted observations of the galactic plane using FRMs during the austral winter of 2006. Several hundred hours of data were taken with the FRMs biased with a 1 Hz square wave. This modulation waveform effected $\pm 45°$ of polarization angle rotation. Other modulation waveforms can provide more or less rotation, as desired. To validate the FRM technology we targeted several bright regions of the galactic plane. Results from some of these observations are displayed in Figure 6, where we also show the same region as imaged by WMAP.[16]

5. CONCLUSIONS

The Faraday Rotation Modulator described in this white paper represents a new form of polarization modulation. Due to its wide-bandwidth performance, high modulation rate, and ability to operate at cryogenic temperatures it is uniquely capable as a polarization modulator for CMB applications. The solid-state nature of the device

combined with the ability to mass-produce devices also implies it is suitable for array applications – sure to be an essential component of all future probes of the polarization of the Cosmic Microwave Background radiation.

6. ACKNOWLEDGMENTS

This project has been supported by the Caltech President's Fund and by the University of California, San Diego and NSF PECASE Award # AST-0548262. Evan Bierman assisted in the design, development, and fabrication of the FRMs used in BICEP. Thomas Renbarger and Evan Bierman provided figures used in this paper. Ed Wollack and Neal Erickson provided many useful insights as well as assisting with design considerations. Helpful comments from Jamie Bock, Darren Dowell, William Jones, Chao-lin Kuo, Andrew Lange, and Ki Won Yoon are gratefully acknowledged.

REFERENCES

1. B. G. Keating, C. W. O'Dell, J. O. Gundersen, L. Piccirillo, N. C. Stebor, and P. T. Timbie, "An Instrument for Investigating the Large Angular Scale Polarization of the Cosmic Microwave Background," *Astrophysical Journal Supplement Series*, vol. 144, pp. 1–20, Jan. 2003.
2. K. W. Yoon, P. A. R. Ade, D. Barkats, J. O. Battle, E. M. Bierman, J. J. Bock, J. A. Brevik, H. C. Chiang, A. Crites, C. D. Dowell, L. Duband, G. S. Griffin, E. F. Hivon, W. L. Holzapfel, V. V. Hristov, B. G. Keating, J. M. Kovac, C. L. Kuo, A. E. Lange, E. M. Leitch, P. V. Mason, H. T. Nguyen, N. Ponthieu, Y. D. Takahashi, T. Renbarger, L. C. Weintraub, and D. Woolsey, "The Robinson Gravitational Wave Background Telescope (BICEP): a bolometric large angular scale CMB polarimeter," in *Millimeter and Submillimeter Detectors and Instrumentation for Astronomy III. Edited by Zmuidzinas, Jonas; Holland, Wayne S.; Withington, Stafford; Duncan, William D.. Proceedings of the SPIE, Volume 6275, pp. 62751K (2006).*, ser. Presented at the Society of Photo-Optical Instrumentation Engineers (SPIE) Conference, vol. 6275, Jul. 2006.
3. E. M. Leitch, J. M. Kovac, C. Pryke, J. E. Carlstrom, N. W. Halverson, W. L. Holzapfel, M. Dragovan, B. Reddall, and E. S. Sandberg, "Measurement of polarization with the Degree Angular Scale Interferometer," *Nature*, vol. 420, pp. 763–771, Dec. 2002.
4. N. Caderni, R. Fabbri, B. Melchiorri, F. Melchiorri, and V. Natale, "Polarization of the microwave background radiation. II. An infrared survey of the sky," *Phys. Rev. D*, vol. 17, pp. 1908–1918, Apr. 1978.
5. A. G. Murray, A. M. Flett, G. Murray, and P. A. R. Ade, "High efficiency half-wave plates for submillimetre polarimetry," *Infrared Physics*, vol. 33, pp. 113–125, 1992.
6. R. H. Hildebrand, J. A. Davidson, J. L. Dotson, C. D. Dowell, G. Novak, and J. E. Vaillancourt, "A Primer on Far-Infrared Polarimetry," *Publications of the Astronomical Society of the Pacific*, vol. 112, pp. 1215–1235, Sep. 2000.
7. P. M. Lubin and G. F. Smoot, "Search for linear polarization of the cosmic background radiation," *Physical Review Letters*, vol. 42, pp. 129–132, Jan. 1979.
8. B. G. Keating, P. A. R. Ade, J. J. Bock, E. Hivon, W. L. Holzapfel, A. E. Lange, H. Nguyen, and K. Yoon, "BICEP: a large angular scale CMB polarimeter," in *Polarimetry in Astronomy. Edited by Fineschi, Silvano. Proceedings of the SPIE, Volume 4843, pp. 284-295 (2003).*, Feb. 2003, pp. 284–295.
9. B. R. Johnson, J. Collins, M. E. Abroe, P. A. R. Ade, J. Bock, J. Borrill, A. Boscaleri, P. de Bernardis, S. Hanany, A. H. Jaffe, T. Jones, A. T. Lee, L. Levinson, T. Matsumura, B. Rabii, T. Renbarger, P. L. Richards, G. F. Smoot, R. Stompor, H. T. Tran, C. D. Winant, J. H. P. Wu, and J. Zuntz.
10. P. Timbie and G. Tucker, "Adding Interferometry for CMBPol," *this volume*, Aug. 2008.
11. G. P. Nanos, "Polarization of the blackbody radiation at 3.2 centimeters," *Astrophysical Journal*, vol. 232, pp. 341–347, Sep. 1979.
12. C. E. Barnes, "Broad-band Isolators and Variable Attenuators for Millimeter Wavelengths," *IEEE Trans. Microwave Theory Tech.*, vol. 9, p. 519, 1961.
13. N. R. Erickson, "Very Low Loss Wideband Isolators for Millimeter Wavelengths," *IEEE Trans. Microwave Theory Tech.*, vol. 1, p. 1, 2001.

14. W. C. Jones, R. Bhatia, J. J. Bock, and A. E. Lange, "A Polarization Sensitive Bolometric Receiver for Observations of the Cosmic Microwave Background," in *Millimeter and Submillimeter Detectors for Astronomy. Edited by Phillips, Thomas G.; Zmuidzinas, Jonas. Proceedings of the SPIE, Volume 4855, pp. 227-238 (2003).*, Feb. 2003, pp. 227–238.
15. G. P. J. Nanos, "Polarization of the Blackbody-Radiation at 3.2 cm." *Ph.D. Thesis*, 1974.
16. L. Page, G. Hinshaw, E. Komatsu, M. R. Nolta, D. N. Spergel, C. L. Bennett, C. Barnes, R. Bean, O. Doré, J. Dunkley, M. Halpern, R. S. Hill, N. Jarosik, A. Kogut, M. Limon, S. S. Meyer, N. Odegard, H. V. Peiris, G. S. Tucker, L. Verde, J. L. Weiland, E. Wollack, and E. L. Wright, "Three-Year Wilkinson Microwave Anisotropy Probe (WMAP) Observations: Polarization Analysis," *Ap. J. Supp. Ser.*, vol. 170, pp. 335–376, Jun. 2007.